

Simulation of electron beam welding of 316L stainless steel thin plates

[Elena Koleva, Lilyana Koleva, Georgi Mladenov, Tsvetomira Tsonevska, Dmitriy Trushnikov]

Abstract — In this paper the simulation of electron beam welding of thin 316L stainless steel thin plates by a moving linear heat source is considered. Regression models for the molten pool geometry characteristics, depending on the electron beam power and the welding velocity are estimated. The thermal histories and the cooling rates defining the microstructure and the distribution of the mechanical properties of the welded samples are also estimated. The influences of the initial temperature T_0 and the welded sample thickness on the temperature distributions are demonstrated.

Keywords — electron beam welding, stainless steel 316L, heat model, linear heat source

I. Introduction

The electron beam welding has been developed over the years into a flexible and economic manufacturing tool [1] for implementation in numerous industries such as automotive, military, aviation and others. The advantages of the process are

the following: it is typically performed in high vacuum, which prevents the heated and melted material from oxidizing and from interactions with atmosphere's pollutions, thus giving the possibility to process reactive metals and their alloys (titanium, etc.); the high power density of the electron beam allows processing of refractory metals and alloys (such as tungsten, molybdenum, niobium, etc.); due to the deep penetration in the work-piece, the electron beam is able to generate narrow weld with minimal thermally-affected zone and without the usage of welding consumables. The geometry of the molten pool [2] and the thermally affected zone, as well as the occurrence of defects [3] and the change of the mechanical properties [4, 5] of the welded samples depend on a large number of parameters, describing the processed material, the characteristics of the electron beam equipment, as well as the technological process itself.

The complex interactions between energy flows and the treated material, as well as the not enough cleared mechanism of electron beam penetration and the complex dynamics of the molten liquid bath, lead to incomplete physical models regarding beam penetration and heat transfer. Nevertheless, different model-based simulations of the process are very helpful for the initial choice of welding parameters (electron beam power, welding velocity, processing spot size, etc.) depending on: the welded material (or materials); the dimensions of the welded samples; the temperature distributions and gradients, connected with the changes in the crystal structure and the mechanical properties of the samples; the requirements for lack of defects and others [6].

The austenitic stainless steel 316/316L is a chromium-nickel-molybdenum alloy with low carbon content, developed to provide improved corrosion resistance in moderately corrosive environments. It has excellent mechanical properties and very good weldability and it is a preferred alloy for various architectural, industrial and transport applications. In [4] an experimental investigation of the influence of electron beam irradiation on the mechanical properties of austenitic stainless steel 316L (SS 316L) 0.5 mm thin samples with different electron beam powers and different irradiation duration is presented. Analogue heating impact is observed during the process of electron beam welding of thin plates in the neighboring regions of the molten pool. This heating is connected with a change in the 0.2% proof strength $R_{p0.2}$, the tensile strength R_m and the percentage elongation after fracture A_{30} . On the other hand, the quality of the welded joint depends on the temperature gradients G at the solid-liquid interface and the local solidification growth rate, R are the most important parameters that affect the solidification structure [6]. The ratio of the parameters, G/R , affects the morphology of the solidification structure and GR , the cooling rate, affects the scale of the microstructure. The shape of the fusion zone and the temperature field affect both G and R , taking into account

Elena Koleva
Institute of Electronics, Bulgarian Academy of Sciences, 72, Tzarigradsko shose, Sofia 1784
University of Chemical Technology and Metallurgy, 8, Kliment Ohridski blvd., Sofia 1756
Bulgaria

Lilyana Koleva
University of Chemical Technology and Metallurgy, 8, Kliment Ohridski blvd., Sofia 1756
Bulgaria

Georgi Mladenov
Institute of Electronics, Bulgarian Academy of Sciences, 72, Tzarigradsko shose, Sofia 1784
Bulgaria

Tsvetomira Tsonevska
Institute of Electronics, Bulgarian Academy of Sciences, 72, Tzarigradsko shose, Sofia 1784
Bulgaria

Dmitriy Trushnikov
Perm National Research Polytechnic University, Perm, Komsomolski Prospekt str.
Russian Federation

that the peak temperature in the molten pool can be several hundred degrees above the liquid us temperature of the material. The rapid heating and cooling leads to sharp peaks in time temperature plots that result in high heating and cooling rates. Depending on the material and the spot location the cooling rates may vary significantly. Also, at very high scanning speeds, the molten pool tends to elongate and can become unstable.

In this paper the simulation of electron beam welding of thin 316L stainless steel 0.5 mm thin plates by a moving linear heat source, using Rosenthal's [7] solution, is considered. Regression models for the molten pool geometry characteristics, depending on the electron beam power and the welding velocity are estimated. The influence of the initial temperature T_0 and the welded sample thickness on the temperature distribution during electron beam welding is also demonstrated. The cooling rates V_c are also calculated.

II. Experimental conditions and simulation results

The solution of the thermal balance steady-state model involving a linear, uniformly distributed heat source in the moving with the beam respectively to sample coordinate system at heating a sheet of thickness h in these conditions assuming no phase changes in the sample during treatment is [8]:

$$T(r, x) = \frac{P}{2\pi\lambda h} \cdot e^{-\frac{Vx}{2a}} \cdot K_0\left(\frac{Vr}{2a}\right) + T_0, \quad (1)$$

where r is radius-vector from the heat source to the studied point, x and y are the coordinates in a moving together with the heat source coordinate system, (x is the axis coinciding with the direction of electron beam movement, y is the distance from this axis), λ and a are the sample thermal conductivity and diffusivity ($a = \lambda/C_p\rho$, where C_p is the specific heat and ρ is the sample density), $K_0(Vr/2a)$ is the modified Bessel function of second kind of order zero, P is the electron beam absorbed energy input (beam energy P_b after correction for energy losses by back scattered and secondary electrons), V is the welding speed, T_0 is the initial sample temperature.

The electron beam welding is performed for 0.5 mm thin stainless steel 316L plates with dimensions 60 mm × 100 mm. Since the plates are thin, the process is performed at higher velocities to avoid the appearance of big molten pools. The chosen regions for the variation of the process parameters are presented in Table 1, where z_1 is power of the electron beam and z_2 is the welding velocity.

TABLE I. PROCESS PARAMETER VARIATION REGIONS

Factor z_i	Dimension	Coded	Lower level ($z_{min,i}$)	Upper level ($z_{max,i}$)
z_1	kW	x_1	0.60	0.90
z_2	mm/sec	x_2	15	25

The coded designations of the process parameters are given in Table 1. The transformation from natural (z_i) to coded (x_i) in the range from -1 to 1 and dimensionless values of the process parameters is done by using the formula:

$$x_i = \frac{2z_i - (z_{max,i} + z_{min,i})}{z_{max,i} - z_{min,i}} \quad (2)$$

In order to investigate the change in the temperature distributions in the samples of thin sheet metal specimens of 316L stainless steel [4], different sets of the process parameters electron beam power (z_1) and welding velocity (z_2) are used. For the simulated experiments, full factorial design with 3 levels of the process parameters is chosen and presented in coded and natural values in Table 2. The initial temperature T_0 for all experiments is 20 °C.

TABLE II. EXPERIMENTAL DESIGN AND OBTAINED RESULTS FOR THE GEOMETRIC CHARACTERISTICS OF THE MELTED ZONE DURING EBW PROCESS

№	Coded values		Natural values		Welding pool geometry			
	x_1	x_2	z_1	z_2	y_1	y_2	y_3	y_1/y_2
1	-1	-1	0.60	15	18.3	4.16	2.08	4.40
2	1	-1	0.90	15	40.7	6.32	3.16	6.44
3	-1	1	0.60	25	11.0	2.49	1.25	4.42
4	1	1	0.90	25	24.4	3.79	1.90	6.44
5	-1	0	0.60	20	13.7	3.12	1.56	4.39
6	1	0	0.90	20	30.5	4.74	2.37	6.43
7	0	-1	0.75	15	28.4	5.24	2.62	5.42
8	0	1	0.75	25	17.0	3.14	1.57	5.41
9	0	0	0.75	20	21.3	3.83	1.97	5.56

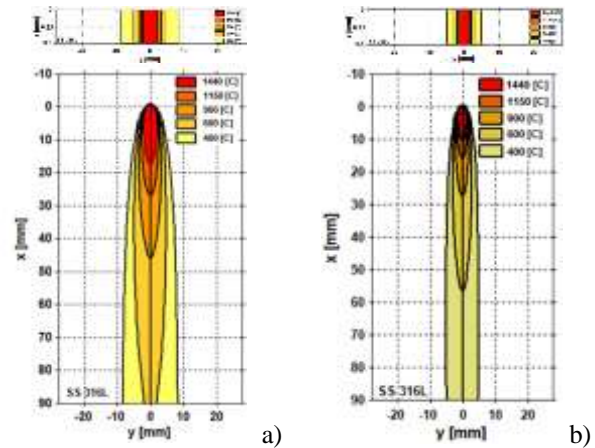


Figure 1. Simulation of electron beam welding of SS 316L in transverse cross-section – y, z – plane and x, y – plane with: a) electron beam power of 600 W, welding speed 15 mm/sec, b) electron beam power of 600 W, welding speed 25 mm/sec.

The obtained results for the geometrical characteristics of the molten pool: y_1 – molten pool length (mm) along the axis x , y_2 – molten pool width (mm) along the axis y and y_3 – molten pool transverse cross-section area (mm^2) in y - z plane are presented in Table II. The ratio molten pool length/width is also calculated. The melting temperature of 316L steel is $T_m = 1400$ °C ($T_S = 1360$ °C, $T_L = 1410$ °C [9]). The thermo-physical properties of stainless steel 316L samples: thermal conductivity λ , thermal diffusivity a , the specific heat C_p and density ρ are temperature-dependent and models for these properties for different temperature regions are estimated in [10]. They are implemented for the simulations of the temperature distributions in the welded samples. Fig. 1 presents the temperature distribution in two SS 316L samples during electron beam welding in the transverse cross-section in y - z plane and in x - y plane with electron beam power of 600 W and welding speeds 15 mm/sec and 25 mm/sec (experiments 1 and 3 from Table 1).

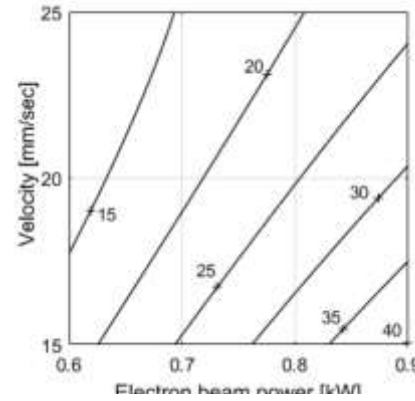
III. Modelling of the geometrical characteristics of the molten zone

The experimental results for the molten pool geometry in Table 2 are used for the estimation of regression models giving the relationship of the geometrical characteristics and the process parameters electron beam power x_1 and the welding velocity x_2 (coded values). They are given in Table 3, together with the values of the corresponding determination coefficients R^2 (the square of the multiple correlation coefficient R) and the adjusted determination coefficients R^2_{adj} . These coefficients are tested for significance and their values are measures for the accuracy of the estimated models. From Table 3 it can be seen that all regression models are very good, the values of their determination coefficients R^2 and the adjusted determination coefficients R^2_{adj} are significant and consequently they are good for prediction and optimization of the considered geometrical characteristics.

TABLE III. REGRESSION MODELS

	Regression models	R^2 , %	R^2_{adj} , %
y_1	$21.833 + 8.767x_1 - 5.833x_2 + 1.467x_2^2 - 2.250x_1x_2$	99.72	99.43
y_2	$3.8967 + 0.8467x_1 - 1.0500x_2 + 0.2933x_2^2 - 0.2150x_1x_2$	99.91	99.81
y_3	$1.96667 + 0.40500x_1 - 0.52333x_2 + 0.13x_2^2 - 0.10750x_1x_2 + 0.02750x_1x_2^2$	99.99	99.99

For verification of the estimated models, another experiment is performed under the same initial conditions and input parameters: plate thickness - 0.5 mm; initial sample temperature $T_0 = 20$ °C; power of the electron beam – $z_1 =$



0.8625 kW ($x_1 = 0.75$) and welding velocity – $z_2 = 16.25$ mm/sec ($x_2 = -0.75$). The results of the performed verification experiment are shown in Table 4.

TABLE IV. VERIFICATION RESULTS

Simulation			Regression models		
y_1	y_2	y_3	y_1	y_2	y_3
34.5	5.58	2.79	34.88	5.61	2.81

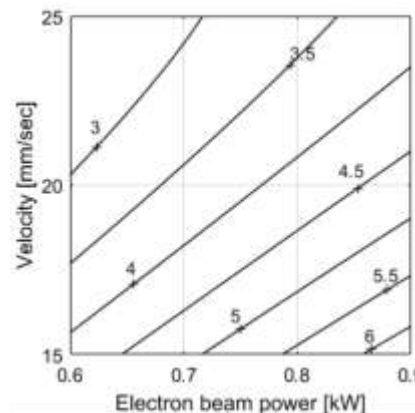
In Figs. 3-5 contour plots of the dependence molten pool width - y_1 (mm), molten pool length – y_2 (mm) and the molten pool transverse cross-section area – y_3 (mm^2) on the variation of the electron beam welding process parameters – electron beam power (z_1) and the welding velocity (z_2) are presented.

Figure 2. Contour plot of the molten pool width - y_1 (mm), depending on electron beam power (z_1) and velocity (z_2).

Figure 3. Contour plot of the molten pool length – y_2 (mm), depending on electron beam power (z_1) and velocity (z_2).

Figure 4. Contour plot of the molten pool transverse cross-section area – y_3 (mm^2), depending on electron beam power (z_1) and velocity (z_2).

It can be seen how the increase of electron beam power increases the molten pool dimensions and on the opposite the increase in welding velocity results in molten pools with reduced dimensions.



IV. Influence of other parameters

The cooling rates $V_c = dT/dt$ (where T is the temperature, t is the time) can be approximately estimated from the calculated thermal cycle. The cooling rates are measured or calculated between the liquidus and the solidus temperatures ($V_{c\ L-S}$) of the material at a location directly below the central axis of the heat source. For electron beam welding the values are typically in the range $10^2 - 10^4$ K/s.

The cooling rates from the liquidus to solidus temperature are used for determining the features of solidification microstructure such as cells and dendrites [11]. The thermal history can be important for determining the extent of solid-state transformations, which vary significantly from one material to another.

Fig. 5 shows the temperature history in a point below the central axis of the electron beam heat source at welding with electron beam power 600 W and welding velocity 15 mm/sec (Experiment 1).

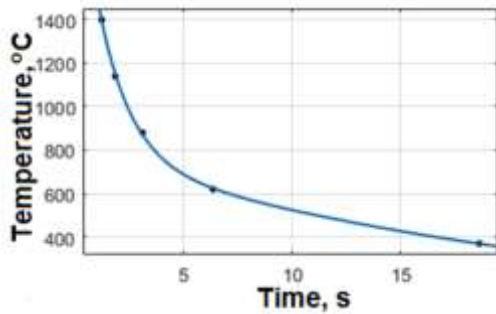


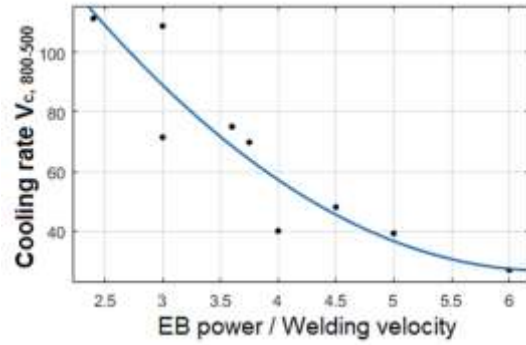
Figure 5. Temperature history in a point below the central axis of the electron beam heat source at welding with electron beam power 600 W and welding velocity 15 mm/sec.

The most important temperature range for steels is the 800 – 500 °C ($V_{c\ 800-500}$) where the cooling rate significantly affects the microstructure and the mechanical properties [12].

The cooling rates depend on the ratio of the electron beam power (energy input) and the welding velocity (z_1/z_2). In [12] it is shown, that the decrease of this ratio leads to decrease of the microhardness and to an increase of the ferrite percentage of the welded samples. The calculated dependence of the cooling rate $V_{c\ 800-500}$ on the ratio of the input power/welding velocity for the performed experiments (Table 2) is presented in Fig. 6.

The initial temperature T_0 also influences the temperature distributions at electron beam welding. In Fig. 7 are presented the results from the simulations for the dimensions of the molten pool length (Fig. 7a) and molten pool width (Fig. 7b) for different values of the initial temperature T_0 and two welding velocities 15 mm/sec and 25 mm/sec. The simulated temperature distribution for electron beam power 600 W and welding velocity 15 mm/sec and initial temperature $T_0 = 200$ °C is presented in Fig. 8a. There the molten pool length is 24.1 mm, the molten pool width is 4.81 mm and the molten pool transverse cross-section area is 2.4 mm^2 .

Figure 6. Dependence of the cooling rate $V_{c\ 800-500}$ on the ratio of the input



power/welding velocity.

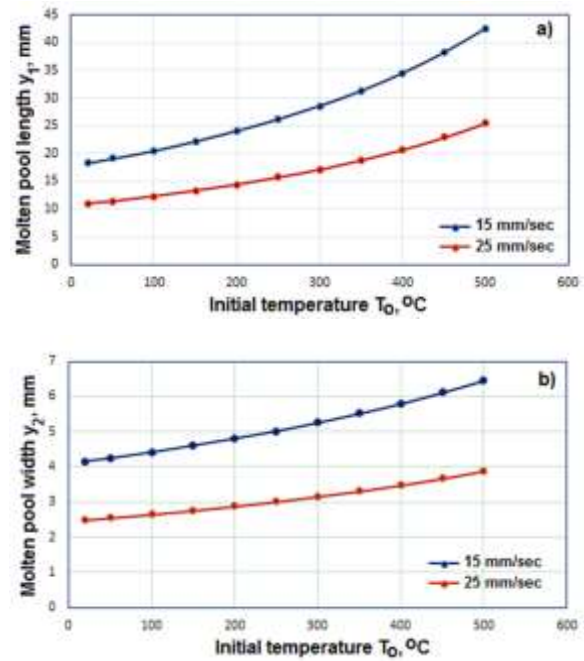
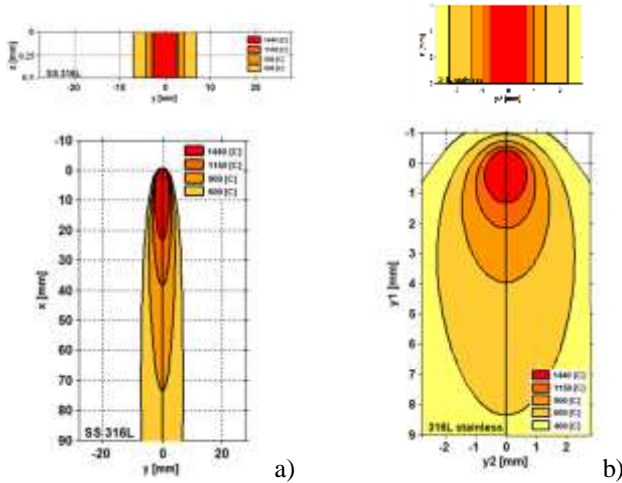


Figure 7. Molten pool a) length and b) width at welding with electron beam power 600 W and welding velocities 15 mm/sec and 25 mm/sec.

The influence of the sample thickness on the geometry of the molten pool is demonstrated on Fig. 8b. There assuming again moving linear heat source the experiment was performed



with plates 3 mm thick, electron beam power of 600 W, welding speed 15 mm/sec and initial temperature 20 °C. There the molten pool length is 1.76 mm, the molten pool width is 1.4 mm and the molten pool transverse cross-section area is 4.2 mm². The dimensions of the plate are again 60 mm × 100 mm, but on the figure is presented reduced part of the surface (6 mm × 10 mm).

Figure 8. Simulation of electron beam welding of SS 316L in transverse cross-section – y,z – plane and x,y – plane of with: a) electron beam power of 600 W, welding speed 15 mm/sec, plate thickness 0.5 mm, initial temperature 200 °C, b) electron beam power of 600 W, welding speed 15 mm/sec, plate thickness 3 mm, initial temperature 20 °C.

v. Conclusion

In this paper, the simulation of electron beam welding of thin 316L stainless steel 0.5 mm thin plates by a moving linear heat source is considered. Full factorial design is used for investigation of the influence of the process parameters the electron beam power and the welding velocity on the geometrical characteristics of the molten pool – length, width and the transverse cross-section. Regression models are estimated for the molten pool geometry characteristics. The influence of other parameters - the initial temperature T_0 and the welded sample thickness - on the temperature distribution during electron beam welding is also demonstrated. The cooling rates temperature range for steels is the 800 – 500 °C ($V_c 800-500$) are calculated for the performed experiments and the dependence on the ratio of the input power/welding velocity is presented.

This paper points that the use of simulated experiments combined with experimental investigations on the mechanical, structural and chemical properties of the welded samples allows to perform investigations of the process electron beam welding at a different scale.

Acknowledgment

The work has been supported by the Bulgarian National Scientific Fund under contract KP-06-N27/18.

References

- [1] E. G. Koleva and G. M. Mladenov, “Experience on electron beam welding. Practical Aspects and Applications of Electron Beam Irradiation Transworld Research Network”, India, Editors: Monica R. Nemtanu and Mirela Brasoveanu, pp. 94-134, ISBN: 978-81-7895-541-4, 2011
- [2] T. S. Tsonevska, E. G. Koleva, L. S. Koleva and G. M. Mladenov, “Modelling the shape of electron beam welding joints by neural networks”. Journal of Physics: Conference Series (<http://jpcs.iop.org>) vol. 1089, 012008, 2018
- [3] L. Koleva and E. Koleva, „Neural networks for defectiveness modeling at electron beam welding“. Industry 4.0, vol. 1/2017, pp. 5-8, 2017
- [4] V. Dzharov, E. Koleva, V. Vassileva, R. Yordanova and S. Yankova, “Modelling of the mechanical properties of steel 316L after EB treatment,” Journal of Physics: Conference Series, vol. 1089 (1), 012004, 2018
- [5] G. Angella, G. Barbieri, R. Donini, R. Montanari, M. Richetta and A. Varone, „Electron beam welding of IN792 DS: effects of pass speed and PWHT on microstructure and hardness“, Materials, Vol. 10, 1033, 2017
- [6] E. G. Koleva, L. S. Koleva and G. M. Mladenov. “Model-based optimization of electron beam welding for obtaining defect-free welds”. Electrotechnica & Electronica E+E, vol. 52. No 3-4/2017, pp. 22-28, 2017
- [7] J. W. Elmer, S. M. Allen and T. W. Eagar, “Microstructural development during solidification of stainless-steel alloys”. Metall Trans A. vol. 20(10), pp. 2117–2131, 1989
- [8] D. Rosenthal, “The Theory of Moving Sources of Heat and Its Application to Metal Treatments,” Transactions of the ASME, pp. 849-866, November 1946
- [9] K. C. Mills, “Recommended values of thermophysical properties for selected commercial alloys”, National Physical Laboratory and ASM International Woodhead Publishing Limited (Cambridge: England), 2002
- [10] E. Koleva, T. Tsonevska, L. Koleva, K. Vutova, G. Mladenov, M. Naplatanova, D. Trushnikov and S. Varushkin, “Simulation of the thermal distribution at electron beam surface modification of stainless steel 316L samples”. Int. Conf. VEIT, Sozopol, Bulgaria, 2019, Journal of Physics: Conference series, 2020, in press.
- [11] H. Yin and S. D. Felicelli, “Dendrite growth simulation during solidification in the LENS process”. Acta Mater, vol. 58(4), pp. 1455–65, 2010
- [12] B. Joseph, D. Katherasan, P. Sathiyal and C. Murthy, “Weld metal characterization of 316L(N) austenitic stainless steel by electron beam welding process”. International Journal of Engineering, Science and Technology. Vol. 4, No. 2, pp. 169-176, 2012

About Authors:



Assoc. Prof. Dr. Eng. Elena G. Koleva
Institute of Electronics, Bulgarian Academy of Sciences, Bulgaria, 72 Tzarigradsko shosse blvd., 1784 Sofia, Bulgaria

Assoc. Prof and lecturer at University of Chemical Technology and Metallurgy – Sofia, Bulgaria.

Scientific research areas: electron beam technologies – welding, melting and refining, lithography, selective melting, surface modification, electron beam characterization, automation, modeling, optimization, standardization.



Dipl. Mag. Tsvetomira S. Tsonevska -
PhD student to IE – BAS, Bulgaria.

Area of Interest: improving and optimization technological and electron beam processes on the basis of statistical methods and optimization. She is currently working at chief expert in manufacturing processes in the pharmaceutical company.



Assist. Prof. Mag. Eng. Lilyana St. Koleva - *Assistant at the University of Chemical Technology and Metallurgy, Sofia.*

Fields of interest are: modeling, parameter optimization, automation, electron beam technologies.



Assoc. Prof. Dr. Dmitriy Nikolaevich Trushnikov - *Department of Applied physics, Department of Welding production and technology of construction materials, Perm National Research Polytechnic University, Perm, Russian Federation; Education - 1999 Department of Aerospace, Perm National Research Polytechnic University*

Research Areas – control, monitoring and simulation of electron beam welding.



Corr. Memb. of BAS, Prof. DSc. Georgi M. Mladenov - *Institute of Electronics – Bulgarian Academy of Sciences, Bulgaria.*

Technological Center on Electron Beam and Plasma Technologies and Techniques, Bulgaria.

He is the author of 10 books, 27 inventions and more than 350 articles. His research interests include electron beam microscope accelerators, electron beam technologies, electron device physics, electron beam welding, melting and refining of metals in vacuum, electron spectroscopy simulation, electron lithography, additive technologies vacuum